Proceedings World Geothermal Congress 2020+1
Reykjavik, Iceland, April - October 2021

Hydromechanical Modelling of the Hydraulic Stimulation of a Fault Zone as Deep Geothermal Target

Arnold Blaisonneau[1 *], Julie Maury[1], Antoine Armandine Les Landes[1], Théophile Guillon[1]

[1] BRGM, 3 Avenue Claude Guillemin, 45000 Orléans, France

[*] a.blaisonneau@brgm.fr

Keywords: Deep geothermal system, fault zone, hydraulic stimulation.

ABSTRACT

In the framework of the H2020-DEEPEGS project, the main technological challenge addressed is to optimize the well architecture and stimulation methods for different geological contexts in order to demonstrate the economic and technical viability of the deep geothermal exploitation. One of the two demonstrators, the VDH French doublet, targets a fault zone in the granitic basement, as deep geothermal system in a rifting context (Upper Rhine Graben in eastern France).

This paper aims to conceptualize a fault zone to represent an equivalent hydromechanical behavior. The objective is to keep the major features of the fault zone while simplifying secondary features that will make the model too complex. The question of how to realize such a conceptualization depending on the knowledge of tectonic context, lithology, hydraulic behavior of each part of the fault zone and existing data is addressed. This conceptual model is used to model hydromechanical processes acting during the hydraulic stimulation of a well in such specific fractured context. Thanks to a DFN numerical model, built on the base of the conceptualization step, the efficiency of hydraulic stimulation is tested with respect to the trajectory of the well VDH demonstrator. The results of the simulations are analyzed to get a qualitative response of the stimulated fracture network (most stimulated fractures and an estimated gain of their hydraulic aperture) around the open hole of the well.

1. INTRODUCTION

The exploitation of the deep geothermal resources represents an alternative solution for heat and/or electricity production in order to mitigate the use of high carbon emissions energies and nuclear energy. Indeed, deep geothermal is a huge potential renewable energy non-intermittent and unlimited at the human scale. If its exploitation is quite well developed and admitted in specific favorable areas such as volcanic geological contexts (volcanic arcs, oceanic rifting etc.), in continental Europe its deployment is still dependent to release brakes. As a matter of fact, apart for heat production for individual or collective uses from porous aquifers in sedimentary basins, the required temperature levels are reached deeper in the upper part of the earth crust (between three to ten kilometers). This implies high upstream investments due to the cost of complicated drilling operations necessary to reach the targeted geothermal resource, often in hard crystalline rocks. In addition, once the drillings completed, because of the nature of rocks and geological context, most of the time it is required to enhance the well productivity by using stimulation techniques to reach the exploitation conditions (flow and temperature for the end use). To face both problems of depth and of "natural" productivity of the well, fault zones in a rifting geological context represent an alternative geothermal target. Indeed, because of the specific geological structure of a rift, higher levels of temperature can be reach at lower depths than in other geological contexts due to regional fluids circulations and connection with deeper parts of the earth crust (Armandine Les Landes *et al.* 2019). Moreover, fault zones in such specific tectonic context have more chances to exhibit favorable hydraulic properties to ensure the well productivity. Nevertheless, this last point is not guaranteed and well stimulation techniques such as hydraulic stimulation may be needed (Vidal *et al.* 2016).

In the framework of the H2020-DEEPEGS project, the main technological challenge addressed is to optimize the well architecture and stimulation methods for different geological contexts in order to demonstrate the economic and technical viability of the deep geothermal exploitation (Peter-Borie *et al.*, 2020). One of the two demonstrators, the VDH French doublet, targets a fault zone in the granitic basement in a rifting context (Upper Rhine Graben in eastern France). This study address the modelling of the hydraulic stimulation of the fault zone considering the specificity of such a geothermal target in terms of geometry, tectonic context and well trajectory. In such a complex geological structures, we have to face to the lack of knowledge and data that limit our understanding of the behavior of the geothermal reservoir. For this reason, numerical modelling is useful to test assumptions on the behavior of the different parts of the fault zone and to analyze the qualitative response around the well. Such analysis can help foster the management of the well in order to test different stimulation scenarios and the implementation of other wells in the fault zone by understanding the specific permeability enhancement in the fault zone.

2. HYDROMECHANICAL CONCEPTUALIZATION OF THE FAULT ZONE

In order to simulate physical processes induced by the hydraulic stimulation of a well, one has to make a conceptualization of the deeply complex reality of natural geological objects, such as fault zones. Indeed, we only have a partial knowledge of their behavior because of their size, accessibility and heterogeneous complexity. Such conceptualization depicts the reality of the geological objects in order to build numerical model integrating the main features of the physical problem addressed. In many injection or production problems, the hydromechanical response around the well is modelled considering the rock reservoir as a continuum media; such approaches are even used to address fracture permeability enhancement within the reservoir (Dempsey *et al.* 2015) or fault zone reactivation and induced seismicity within the reservoir and at its boundaries (Rutqvist *et al.* 2013). However, when dealing with the injection inside a fault zone and the processes during its hydraulic stimulation such approaches do not catch primordial features linked with the geological complexity of such fractured systems. For this reason, the hydromechanical

conceptualization of the fault zone aims to reproduce both the geological and geometrical characteristics of the fault zone within a specific tectonic context integrating hydromechanical behavior from data analysis and knowledge extrapolation (from analogs studies or similar geological contexts data acquisition). For the VDH fault zone, Figure 1 explicits the fault conceptual model that illustrates the different parts of the dissymmetric fractured system linked with its tectonic heritage and its localization within the graben (Peter-Borie *et al*. 2020). From the drilling data and fluid inflow measurement, hydraulic behavior of the different parts of the fault zone can be extrapolated. Hence, following the well crossing the fault zone (from left to right in Figure 1) three main compartments can be highlighted:

- the Damage zone (DZ) in which fractures are more or less opened with assumed quite high permeabilities (one main loss at the top of the damage zone and then several minor losses distributed along the damage zone);
- A first part of the Fault core (FC1) representing the fault gauge with sealed discontinuities and assumed low permeability (no losses);
- A second part of the Fault Core (FC2) transmissive with diffusive losses, heavily fractured and brecciated that can be simplified as an area of globally high matrix permeability.

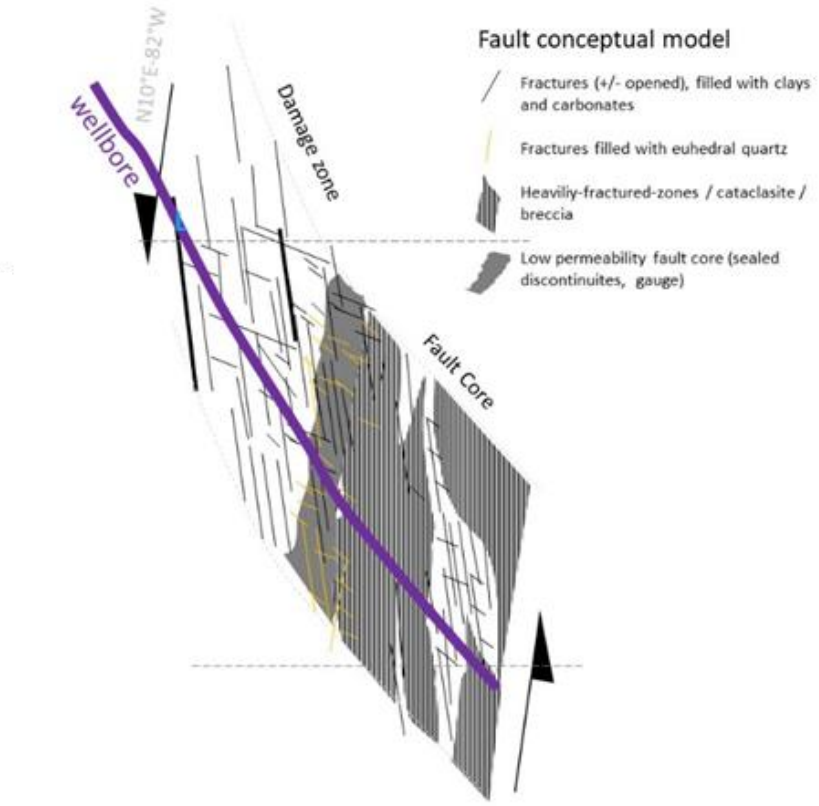

Figure 1: Conceptual model of the geometry of the targeted fault zone based on the drilling data

From a hydraulical point of view, the major interfaces that delineate the three main zones of this fault zone appear favorable to flow (Armandines les landes *et al*. 2020).

Hydraulically this fault zone with three distinct areas can be conceptualized as:

- four structuring fractures heavily permeable
- a DZ with a network of discrete fractures with varying permeability
- an impermeable FC1
- a FC2 equivalent to a single structure heavily permeable represented by the fourth structuring fracture

Without any indications about the mechanical behavior of the different part of the fault zone, the mechanical conceptualization is only based on the opening/sealing of the discontinuities.

3. 3D NUMERICAL MODEL FOR THE HYDRAULIC STIMULATION

In order to simulate the behavior of the fault zone around the open hole of the well during the hydraulic stimulation, a 3D model, based on the previous hydromechanical conceptualization is implemented with the code 3DEC© (Itasca 2016). This code is based on the Distinct Element Method. The numerical model (Figure 2) integrates the fracture model (the fractures are represented by 2D joints) defined in the conceptual model. In the context of our works, numerical procedures have been developed to simulate hydromechanical processes due to fluid flow in deformable joints. Hence, the model can address interactions between mechanical (strains, stresses and displacements) and hydraulical phenomena (fluid pressure, flows and hydraulic apertures) within a rock matrix cut by discontinuities. Joints and blocks (representing rock matrix) are deformable whereas fluid flows only take place inside discontinuities, blocks being consider impermeable. This assumption is suitable for deep fractured geothermal reservoir for which

the matrix permeability of the crystalline rocks (such as granitic rock) is negligible compared to fractures and fault zone permeability.

3.1 3D geometrical model

The 3D model is a cube centered on the open hole of the well in the fault zone of 500 m length for each side. The block, representing the rock matrix, is cut by a discrete fracture network (DFN) illustrating the fracture model of the fault zone (Figure 2). This DFN is based on the conceptual model of the fault zone with the three distinct compartments (DZ, FC1 and FC2), delimited by four structuring fractures heavily permeable (see companion paper Armandine les Landes et al. 2020). In the damage zone (DZ) and the first part of the fault core (FC1), between the structuring fractures, a set of fracture families based on the interpretation with a Riedel model is considered.

A mean mesh size of 19 m is used to model well the structures with a minimum distance between parallel fractures of 23 m. The mesh is a little more refine within the DZ, 16 m, to account for the high number of fractures while avoiding side effect with keeping to values close.

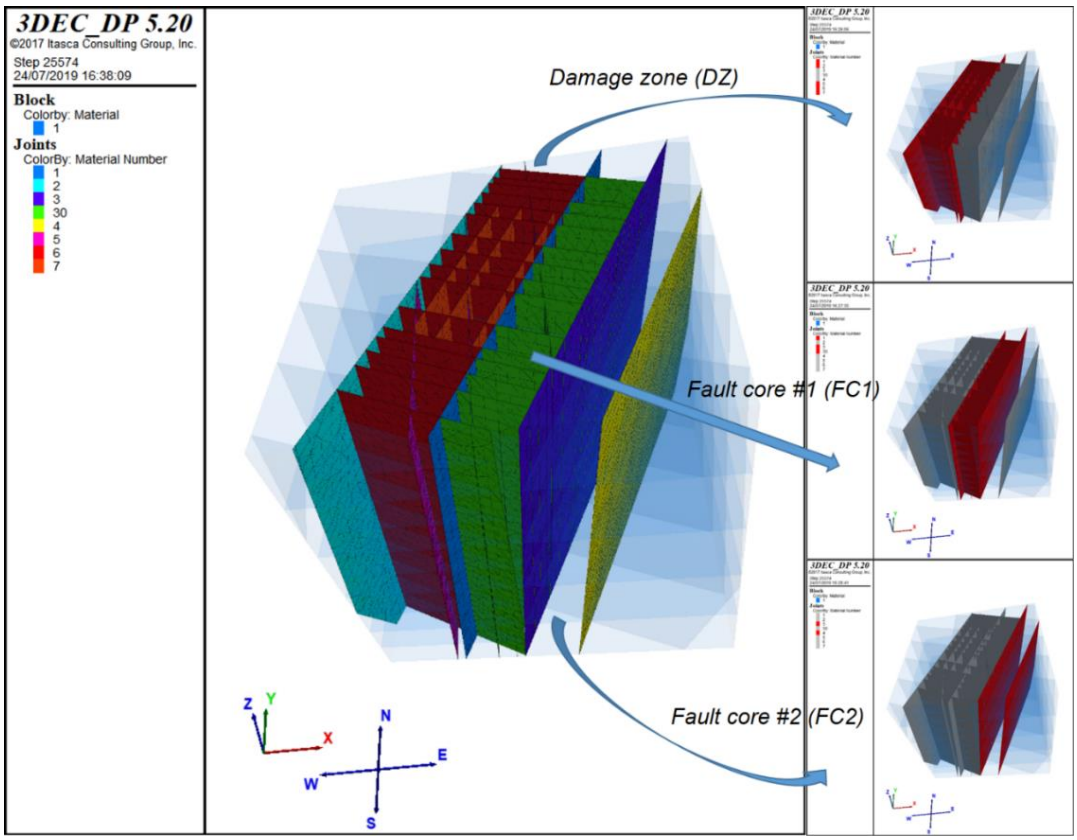

Figure 2: 3D numerical model for the fault zone hydraulic stimulation.

3.2 Initial and boundary conditions

For initial conditions, a 3D *in situ* stress tensor is applied to the model and the hydraulic pressure in the joints is assumed to be hydrostatic (at a depth the pressure is given by the weight of the whole water column upside). The *in situ* stress tensor has been evaluated for the VDH site by the analysis of borehole breakouts with respect to well trajectory and mud losses during the drilling (internal communication). The stress tensor considered is:

$$\sigma_h = 0.6*\sigma_v \qquad \sigma_H = 1.1*\sigma_v \qquad \sigma_v = 0{,}00268*9.81*z \tag{1}$$

where z is the depth in m, σ_h et σ_H respectively the minor and major horizontal principal stresses and σ_v the vertical principal stress. The direction of the major horizontal principal stress σ_H is N160°E.

To apply the stress tensor for initial condition and during simulation for mechanical boundary conditions, mixed boundary conditions are applied to the model boundaries: normal displacements are fixed at South and East faces, whereas the *in situ* principal stress state (eq. 1) loads the West, North and top faces. Bottom face is completely clamped.

3.3 Constitutive behaviors

3.2.1 Mechanical behavior

The impermeable rock matrix is supposed to be isotropic elastic and properties considered for the granitic matrix blocks in the model are listed in table 1:

Table 1 – Mechanical properties for granitic matrix.

Density (kg/m^3)	Young's modulus (MPa)	Poisson ratio
2680	52000	0,29

The constitutive mechanical joints model aims at reproducing the dilatant behavior of hydromechanically active joints. Joints are described using a Coulomb criterion where a yield shear stress controls the onset of slipping:

$$\begin{cases} \tau_s = k_s u_s & u_s \le \tau_{max} / k_s \\ \tau_s = \tau_{max} & u_s > \tau_{max} / k_s \end{cases} \quad (2)$$

Where τ_{max} [Pa] et k_s [Pa.m^{-1}] are the yield shear stress and the shear tangential stiffness, u_s [m] is the shear displacement.

The yield shear stress depends on the normal effective stress σ_n [Pa] acting on the joint:

$$\tau_{max} = c + \sigma_n \tan\phi \quad (3)$$

where c [Pa] is the fault zone cohesion, and ϕ [°] is the friction angle.

The normal displacement is the sum of an elastic and a dilational components. Dilation occurs at the onset of slipping, and depends on another intrinsic angle, the dilation angle:

$$u_n = u_n^{el} + u_n^{dil} = (\sigma_n + \Delta P)/k_n + \tau_s \tan\psi \quad (4)$$

where u_n [m] is the normal displacement, u_n^{el} and u_n^{d} [m], are its elastic and dilational components, ΔP [Pa] hydraulic overpressure, k_n [Pa.m-1] is the normal stiffness, and ψ [°] is the dilation angle.

As it can be seen on Figure 3, u_n^{d} is bounded by a threshold value to account for the dilation stopping when the residual friction state is reached. The normal effective stress will impact both the yield shear stress τ_{max} and the maximum dilational opening u_n^{d}.

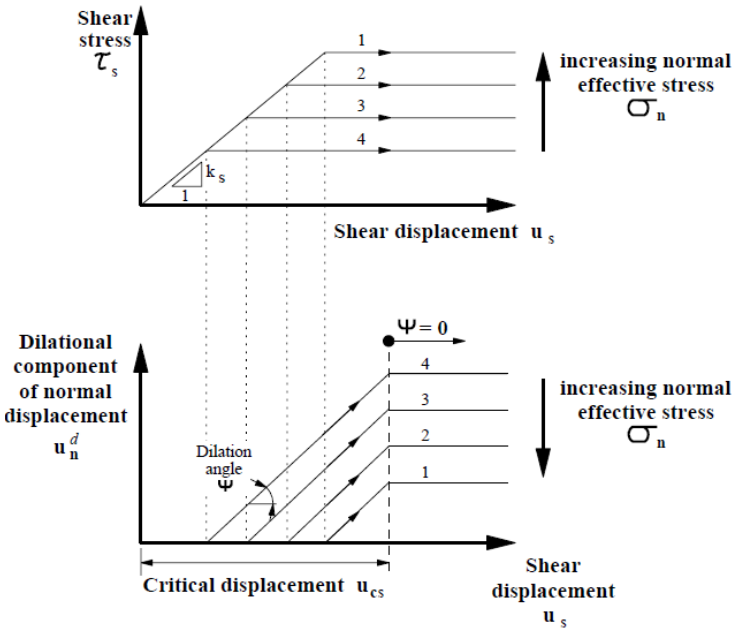

Figure 3: Mohr-Coulomb slip model, example for non-cohesive fault zones (Itasca 2016). The dilational opening is bounded by an upper limit linked to the critical displacement u_{cs}.

A tensile strength is also considered, and contact is lost at the grid points where tensile failure occurred.

Table 2 summarizes joints mechanical parameters considered in the model.

Table 2– Mechanical parameters for joints.

k_n [MPa/m]	k_s [MPa/m]	c [MPa]	ϕ [°]	ψ [°]	u_s^c [mm]
25000	*25000*	0	45	1	10

For the joints inside the impermeable area FC1, the normal and shear stiffness have been increased by a factor ten and 10 MPa cohesion has been considered. This assumption is made in accordance with this area observed to be sealed.

3.2.2 Hydraulic behavior

The fluid flow inside the joints is assumed to be monophasic laminar and can be modelled by the cubic law:

$$Q_f = -\frac{\rho g}{12\mu} a^3 \frac{\Delta h}{L} \tag{5}$$

where Q_f is the flow (m^3/s), for a unit width fracture with an hydraulic aperture a [m], $\Delta h/L$ is hydraulic head gradient for a length L of flow, ρ and μ are respectively the fluid density and the dynamic viscosity, and g the acceleration gravity.

3.2.3 Hydromechanical coupling

The influence of the hydraulic behavior of the fractures on the mechanical behavior directly accounts for the calculus of the normal displacement by the integration of the hydraulic overpressure in (eq. 4). To take into account the influence of the mechanical response in the fracture on the flow, the hydraulic aperture is assumed to be a function of the normal displacement:

$$a = a_0 + u_n \tag{6}$$

where a_0(m) is the initial hydraulic aperture.

To account for the hydraulic conceptualization of the different parts of the fault zone, a set of hydraulic parameters (table 3) is considered, discriminating joints and fracture sets depending on their area in the fault zone.

Table 3– Hydraulic parameters for joints.

FZ area and description	a_0 [mm]
Highly productive structure in DZ	$2\ 10^{-3}$
Productive structure of the fault zone	$5\ 10^{-4}$
Fracture set R (Riedel model) in DZ	$5\ 10^{-4}$
Fracture set R' (Riedel model) in DZ	$1\ 10^{-4}$
Fracture sets in FC1	$1\ 10^{-6}$

3.4 Hydraulic stimulation

The hydraulic stimulation is simulated by applying overpressure values at the set of mesh nodes representing the well and corresponding to the intersection of the joints with the well trajectory (Figure 4). For this study, the following stages of overpressure values (in MPa) have been imposed {0.5; 1; 2; 3; 4; 5; 6; 7; 8; 9; 10}. After this hydraulic stimulation phase, an unloading calculation is performed by progressively decreasing the hydraulic loading in the well and allowing a rebalance of the model. In the end only irreversible processes persist within the model such as, e.g., residual hydraulic apertures due to the dilational opening of the joints.

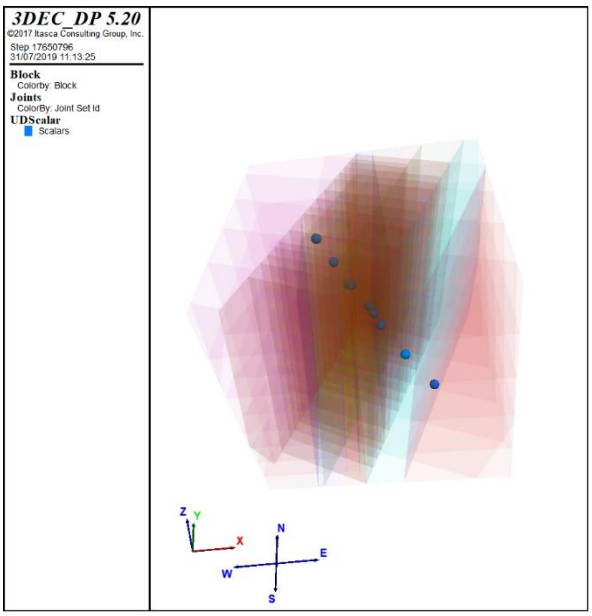

Figure 4: 3D model with injection nodes (blue dots) corresponding to the intersection of the joints with the well trajectory.

4. RESULTS

Figure 5 shows the spatial evolution of main joints variables for the hydraulic overpressure step of 10 MPa. This overpressure imposed at the injections nodes induces a change of joint pore pressure along the well trajectory in the whole fractured system. Because of the different hydromechanical behavior of the joints depending on their fault zone compartment (DZ, FC1 and FC2) and on fracture set, the hydromechanical response of the system is heterogeneous. The FC1, with lower hydraulic apertures and higher joint stiffnesses exhibit a zone where the joint normal displacements are lower (Figure 5 b). The major mechanical changes are located in the DZ (Figure 5 c and d).

The effects of the stimulation phase can been estimated by the results obtained after the well pressure shutdown simulation. Figure 6 shows the contour of the hydraulic aperture after the stimulation and the shutdown depending on the compartment of the fault zone (fault core or damage zone) and the fracture set. Because of their stiffness and their lowest initial aperture, the joints in the impermeable part of the fault core (FC1) have all gained an irreversible hydraulic aperture (Figure 6 a) except at their intersection with productive fractures. Nevertheless, because of their low initial value the hydraulic aperture remains lower than in the joints from other compartments (DZ and FC2). In the damage zone (DZ), all the fracture sets exhibit a zone where the hydraulic aperture has been increased (Figure 6 b, c and d). It appears that these hydraulic aperture gains due to the irreversible changes induced by the hydraulic stimulation are mostly located in the bottom part of the 3D fracture network.

To get a global 3D view of the effect of the hydraulic stimulation within the model, Figure 7 illustrates the 3D halo of the ratio increase of the hydraulic aperture (larger than 10 X the initial hydraulic aperture of the joints). Excepted changes in the FC1, the major changes are located in the part of the DZ in vicinity of the impermeable fault core (FC1), which is acting like an impermeable rigid body that concentrates hydromechanical effects.

To remind, the results analyzed above were obtained with a model considering that for the joints inside the impermeable area FC1, the normal and shear stiffness have been increased by a factor ten and 10 MPa cohesion has been considered. This assumption was made in order to conceptualize the fact that in this FC1 zone, fractures are sealed with competent material (such as hydrothermalized calcite clogging). To see the influence of the mechanical joints parameters of this impermeable fault core FC1, a second model has been run where the normal and shear stiffnesses of the joints in FC1 are two times lower than in other joints in the model. This assumption tends to conceptualize that in this case the impermeable fault core FC1 corresponds to highly brecchified area with argillaceous materials. Figure 8 illustrates the 3D halo of the ratio increase of the hydraulic aperture (larger than 10 X the initial hydraulic aperture of the joints) for this two ways of conceptualizing the mechanical behavior of the joints in FC1 (sealed fractures = rigid behavior, argillaceous brecchia = soft behavior). In case of soft mechanical behavior of the joint in FC1 (Figure 8 b), the gain of hydraulic aperture in the DZ is less pronounced than in the case of rigid behavior (Figure 8 c). This is a consequence of the rigid behavior entering sooner the plastic phase and thus being more prone to triggering high aperture gains (which are linked to irreversible processes). Further work should include not only different parameters for sealed and argillaceous joints, but also different behaviors (fragile and ductile, respectively).

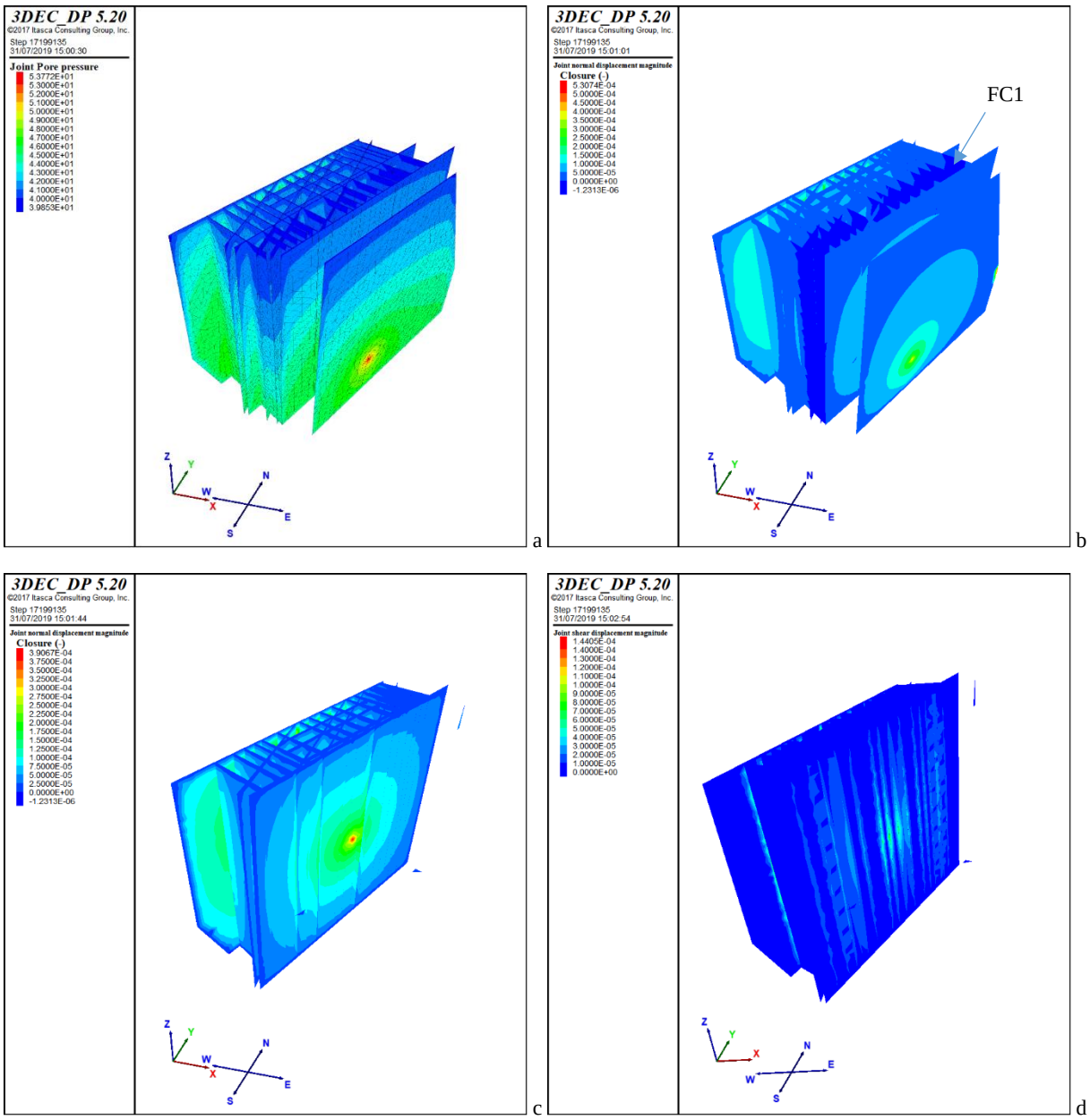

Figure 5: Contours representation of variables for 10 MPa step of the hydraulic stimulation: a/ joint pore pressure, b/ joint normal displacements, c/ joint normal displacements focus on the DZ and d/ joint shear displacements focus on the DZ.

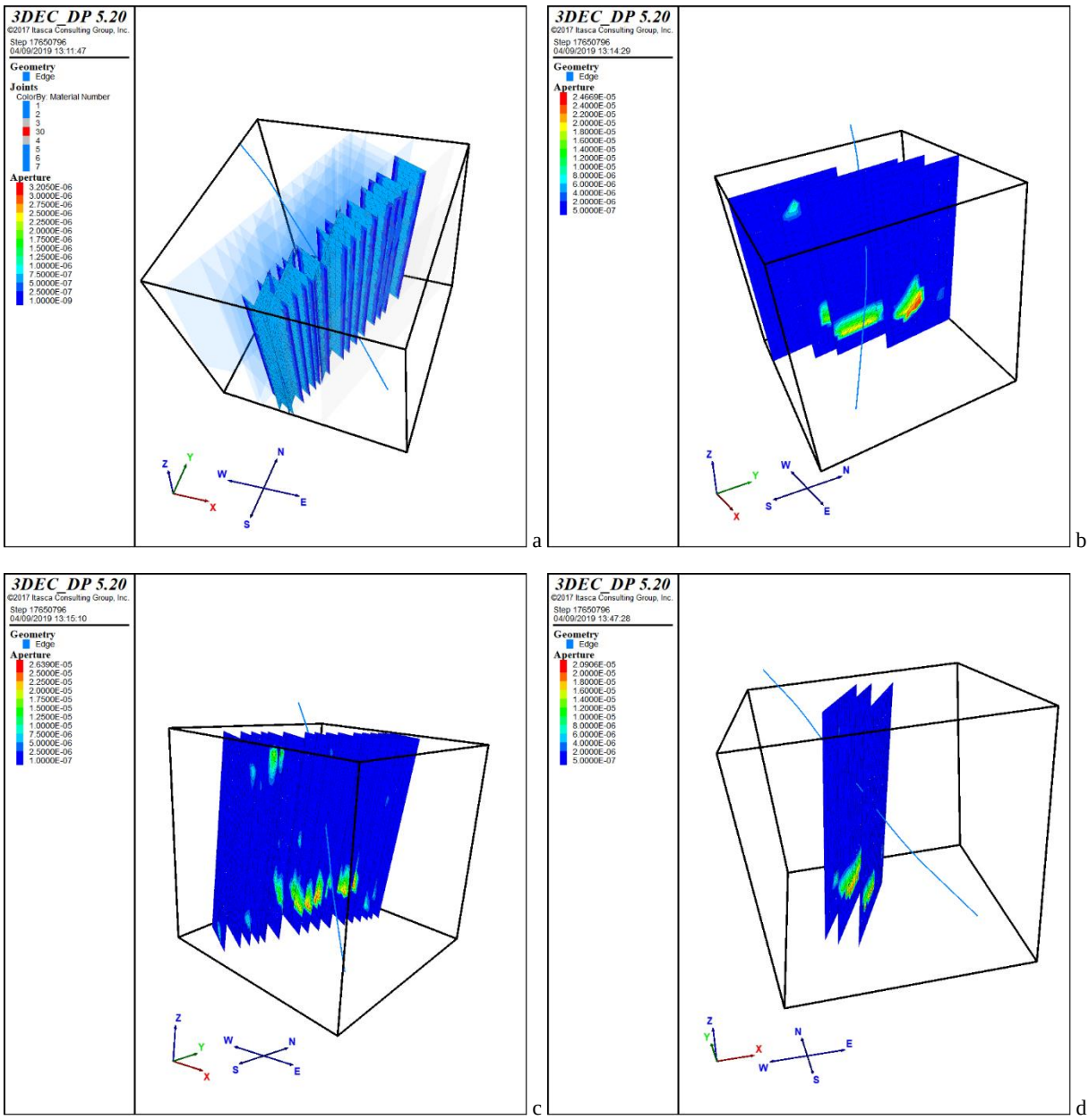

Figure 6: Contours representation of hydraulic apertures after shutdown : a/ in the FC1 zone, b/ in DZ for fracture set R, c/ in DZ for fracture set R' and d/ in DZ for productive fractures.

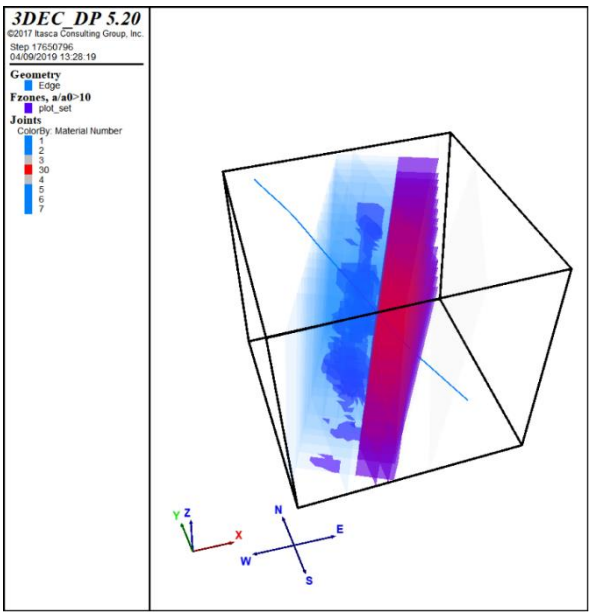

Figure 7: 3D halo of the increase (blue patches) of the hydraulic aperture larger than 10 X the initial hydraulic aperture of the joints (in blue the well trajectory). Transparent blue planes represent the location of the associated fractures.

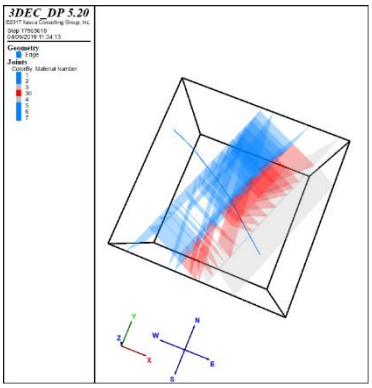
a

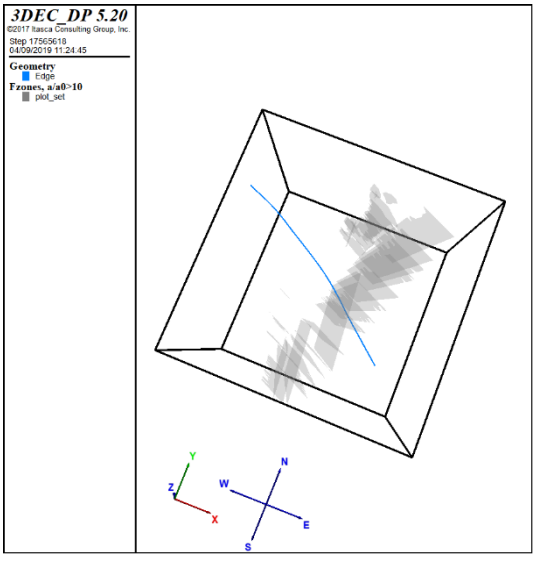

b

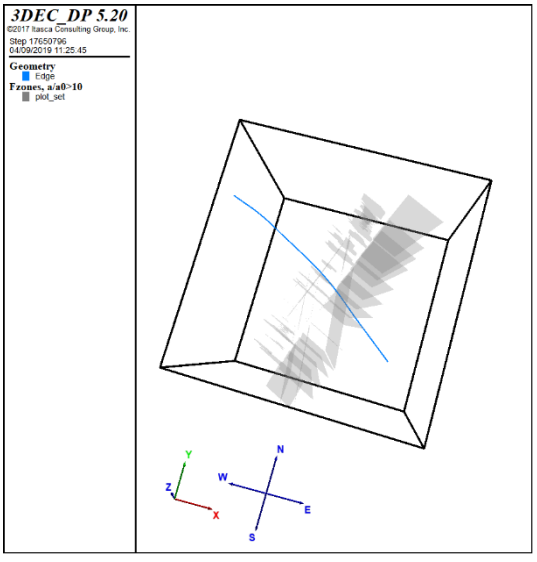

c

Figure 8: 3D halo of the increase of the hydraulic aperture larger than 10 X the initial hydraulic aperture of the joints (a/ reference view of the model with colored zone DZ, FC1, FC2) : b/ FC1 argillaceous brecchia with soft mechanical behavior, c/ FC1 sealed fractures with rigid mechanical behavior.

5. CONCLUSIONS

The modelling works showed in this paper aim at estimate the effects of the hydraulic stimulation of a well intercepting a fault zone in the context of the VDH French doublet. The way to conceptualize such complex 3D geological object in a specific tectonic context is crucial and the model is focused on the conceptualization of different compartments in the fault zone with different hydraulic behavior, based on drilling and flow data, in order to construct a 3D discrete fracture network model. The results highlight the location of gain of hydraulic aperture in the joints and hence the efficiency of the hydraulic stimulation modelled. This gain of hydraulic aperture depends on the location in the fault zone and on the orientation of the fracture sets. The results show the influence of an impermeable compartment (FC1) that focus hydromechanical processes in its vicinity. The way to consider the mechanical behavior in this fault core impermeable compartment has been tested depending on the geological nature of this part of the fault core (sealed fracture versus highly brecchified with clay material).

REFERENCES

Armandine Les Landes, A., Guillon, T., Peter-Borie, M., Blaisonneau, A., Rachez, X., Gentier, S.: Locating Geothermal Resources: Insights from 3D Stress and Flow Models at the Upper Rhine Graben Scale, *Geofluids* Volume 2019, Article ID 8494539, 24 pages (2019).

Armandine Les Landes, A., Maury, J., Guillon, T., Lopez, S., Blaisonneau, A., Tran, V. H., Loschetter, A., Peter-Borie, M.: Hydrothermal Simulation in a Fault Zone: Impacts of Stimulation Methods, *submitted in: World Geothermal Congress 2020*. Reykjavik, Iceland.

Dempsey, D., Kelkar, S., Davatzes, N., Hickman, S., Moos, D.: Numerical modeling of injection, stress and permeability enhancement during shear stimulation at the Desert Peak Enhanced Geothermal System, *International Journal of Rock Mechanics & Mining Sciences* 78 (2015)190–206.

Itasca : 3DEC, Version 5.2, 3 Dimensional Distinct Element Code. User's Guide. Itasca Consulting Group Inc., Minneapolis, MN (2016).

Peter-borie, M., Loschetter, A., Maury, J., DEEPEGS Team: Assessment of Geothermal Well Productivity Improvement Technologies: an Overview from the DEEPEGS Project, *submitted in: World Geothermal Congress 2020*. Reykjavik, Iceland.

Rutqvist, J., Rinaldi, A. P., Cappa, F., Moridis, G. J.: Modeling of fault reactivation and induced seismicity during hydraulic fracturing of shale-gas reservoirs, *Journal of Petroleum Science and Engineering* 107 (2013) 31–44.

Vidal, J., Genter, A., Schmittbuhl, J.: Pre- and post-stimulation characterization of geothermal well GRT-1, Rittershoffen, France: insights from acoustic image logs of hard fractured rock, *Geophys. J. Int.* (2016) 206, 845–860.